

DOE/SERI-8119-3/6
(DE82005642)

**SEQUENTIAL PURIFICATION AND CRYSTAL GROWTH FOR THE
PRODUCTION OF LOW COST SILICON SUBSTRATES**

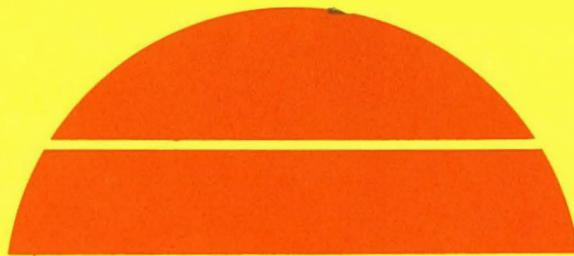
Quarterly Technical Progress Report No. 5 for the Period January 1—March 31, 1981

By
Ming Liaw
Charlie Varker

December 1981

Work Performed Under Contract No. AC02-77CH00178

Motorola, Inc.
Phoenix, Arizona



U.S. Department of Energy



Solar Energy

DISCLAIMER

"This report was prepared as an account of work sponsored by an agency of the United States Government. Neither the United States Government nor any agency thereof, nor any of their employees, makes any warranty, express or implied, or assumes any legal liability or responsibility for the accuracy, completeness, or usefulness of any information, apparatus, product, or process disclosed, or represents that its use would not infringe privately owned rights. Reference herein to any specific commercial product, process, or service by trade name, trademark, manufacturer, or otherwise, does not necessarily constitute or imply its endorsement, recommendation, or favoring by the United States Government or any agency thereof. The views and opinions of authors expressed herein do not necessarily state or reflect those of the United States Government or any agency thereof."

This report has been reproduced directly from the best available copy.

Available from the National Technical Information Service, U. S. Department of Commerce, Springfield, Virginia 22161.

Price: Printed Copy A03
Microfiche A01

Codes are used for pricing all publications. The code is determined by the number of pages in the publication. Information pertaining to the pricing codes can be found in the current issues of the following publications, which are generally available in most libraries: *Energy Research Abstracts, (ERA)*; *Government Reports Announcements and Index (GRA and I)*; *Scientific and Technical Abstract Reports (STAR)*; and publication, NTIS-PR-360 available from (NTIS) at the above address.

SEQUENTIAL PURIFICATION AND CRYSTAL GROWTH
FOR THE
PRODUCTION OF LOW COST SILICON SUBSTRATES

QUARTERLY TECHNICAL PROGRESS REPORT NO. 5
FOR PERIOD
1 JANUARY 1981 - 31 MARCH 1981

MING LIAW, CHARLIE VARKER

DECEMBER 1981

MOTOROLA, INC.
SEMICONDUCTOR PRODUCTS SECTOR
5005 EAST MCDOWELL ROAD
PHOENIX, ARIZONA 85008

UNITED STATES
DEPARTMENT OF ENERGY
DIVISION OF SOLAR TECHNOLOGY
AND
SOLAR ENERGY RESEARCH INSTITUTE
UNDER DOE SUBCONTRACT NO. XS-9-8119-3

THIS TECHNICAL REPORT IS BEING TRANSMITTED IN ADVANCE
OF DOE PATENT CLEARANCE, AND NO FURTHER DISSEMINATION
OR PUBLICATION SHOULD BE MADE OF THE REPORT WITHOUT
PRIOR APPROVAL OF THE DOE PATENT COUNSEL.

MOTOROLA PROJECT NO. 2376

TABLE OF CONTENTS

	Page
List of Tables	
List of Figures	
1.0 Introduction	1
2.0 Experimental Procedures	1
3.0 Experimental Results	3
3.1 Purity of Crystals	3
3.2 Crystal Perfection	6
6 3.2.1 2-pulled crystals	6
3.2.2 3-pulled crystals	9
3.3 Electrical Resistivity and Carrier Mobility	12
3.4 Photoresponse	12
3.4.1 Gated Diodes	12
3.4.2 Silicon wafers with a shallow p-n junction	15
3.4.3 Epitaxy wafers with a p-n junction	18
3.4.4 $I_{SC} \times V_{OC}$ product and predicted maximum	18
4.0 Discussions	18

LIST OF TABLES

	Page
Table 1: Comparison of maximum impurity concentration in 1, 2 and 3-pulled ingots analyzed by spark source mass spectrometer (ppm wt)	4
Table 2: Impurity ratio in Si ingots of each consecutive pull.	5
Table 3: Average short circuit current (I_{SC}) and open circuit voltage (V_{OC}) for diodes illuminated under 5×10^{-3} sun	14
Table 4: Comparison of I_{SC} and V_{OC} of 2 and 3-pulled crystals with those of S.G. wafers of various resistivities (measured under AMI).	16
Table 5: Comparison of I_{SC} and V_{OC} of 3-pulled N ⁺ /P wafers with those of S.G. wafers of various resistivities. (The front of wafers was textured and the back was pt diffused).	17
Table 6: I_{SC} and V_{OC} of N ⁺ diffused wafers (2" dia.) with an epitaxial layer on the substrates of various number of crystal puller.	19

LIST OF FIGURES

	Page
Figure 1: X-ray topograph of a silicon wafer cut from the tang end of a 2-pulled ingot.	7
Figure 2: A higher magnification of Figure (1), (a) center region of the wafer, (b) periphery region of the wafer.	8
Figure 3: Etched surface of the wafers shown in Figure (1) (a) center region, (b) periphery of the wafer.	10
Figure 4: (a) shallow etch pits observed on etch wafer cut from a 3-pulled ingots, (b) shallow etch pits observed on a S.G. wafer.	11
Figure 5: Plot of Hall mobility vs number of crystal pulling	13
Figure 6: Plot of cell efficiency vs $I_{SC} \times V_{OC}$ for various materials.	20

I. INTRODUCTION

The need for low cost silicon for solar cell applications has stimulated the study of direct purification of metallurgical-grade silicon(MG-Si). The technique of sequential purification of molten silicon was investigated.^{1,2} The sequential purification steps included (1) physical separation of insoluble impurities, 2) reactive gas treatment, 3) slagging and 4) impurity redistribution using ingot pulling. The results have shown that the ingot pulling is the most effective step of the purification process. This has been predicted since the majority of metal impurities in silicon have very low segregation coefficients (from 10^{-2} to 10^{-6}). In theory the ingot pulled from the molten silicon will be two to six orders of magnitude lower in the metal concentration than that in the original silicon used for melting. By the same token the pulled ingots can be remelted and repulled. The purity of the silicon can be improved by another 2 to 6 orders of magnitude. The process can be repeated for further purification. The purpose of this paper is to report the purity, structural and electrical characteristics of silicon ingots obtained by various number of crystal pulling.

2. EXPERIMENTAL PROCEDURES

The polycrystalline silicon pulled (1-pull) directly from the MG-Si melts was used as feed stock for second crystal pulling (2-pull). The 1-pulled ingots contain non-uniform distribution of grain size along the crystal axis¹⁻². The seed end contains large grains with polygonal structure, while the tang end contains small grains with lamellar structure. The metallic impurities at the seed end are in the range of tens of ppm, while at the tang end are hundreds of ppm.

The 2-pulled ingots have also been used as feedstock for the additional pull (3-pull). The percents of melt pulled are approximately 60%, 80% and 85% for 1, 2, and 3-pulled crystals respectively. An NRC crystal puller was used with a melt size of 2 Kg. Occasionally a Hamco 800 crystal puller was used for a larger melt size (4 Kg). The NRC puller produced 5.5 cm diameter crystals, while the Hamco produced 7.5 cm diameter crystals. The crystals were pulled along the <100> direction. The crystal growth was done in an argon ambient at one atmosphere pressure. The pull rate was in the range of 6 to 8 cm/hr. The crystal rotation rate was 19 rpm while crucible rotation rate was 7rpm.

The impurity concentration in silicon was measured by the spark source mass spectrometer. The structure of silicon wafers was characterized by chemical etching/optical microscopic method and by X-ray topographic technique. A 4-point probe was used for the measurement of electrical resistivity. The majority carrier mobility was measured by the van der Pauw method.

Silicon wafers were further characterized by the formation of a p-n junction for photoresponse measurement. The junction was made by solid state diffusion of phosphorus impurity either directly into the silicon substrate or into the epitaxial layer. The sheet resistance of the N⁺ layer is in the range of 20 to 40 Ω/sq. The junction depth is approximately 0.3 μm. When an epitaxial layer is applied, it is 20 μm thick with a resistivity of 2.5 Ωcm.

Two different types of devices were built for photoresponse measurement: (1) gated diodes with a size of $4.2 \times 10^{-3} \text{ cm}^2$ per diode. 2) uncomplete solar cells with the sizes of one cell/wafer. The solar cells were only processed up to diffusion and mesa etch. Neither metallization nor AR coating was applied. Open circuit voltage (Voc) and short circuit current (Isc) were taken under a vertical illumination condition (AMI). The products of Voc and Isc is used as a parameter for the material evaluation.

3. EXPERIMENTAL RESULTS

3.1 Purity of Crystals

Two crystal from 1-pulled, four each from 2-pulled and 3-pulled ingots have been analyzed by spark source mass spectrometer. Table 1 lists the maximum impurity concentration found at the seed and tang ends of crystals. The concentration of impurities at the seed end of 1-pulled crystals is comparable with that at the 2-pulled or 3-pulled crystals with the exceptions of Fe, Al and C. This results agree with the previous finding analyzed by the emission spectrographs. The high concentration of impurities at the tang end of 1-pulled crystals is primarily due to the samples with a lamellar grain structure, which is due to the constitutional supercooling during the crystal pulling. The table also shows that the purity of ingots is progressively improved by each additional crystal pulling. However, the improvement in the 3-pulled ingots over 2-pulled ingots is not as dramatic as expected. This is probably due to the fact that the concentration in the 2-pulled crystals already approaches the deflection limit of the instrument. The improvement in purity by each additional crystal pulling can be easily analyzed by taking the concentration ratio of two consecutively pulled crystals. Table 2 lists the ratio for the predominate elements found in MG-Si. This table shows that the second-pull effectively improves the purity at the tang end of crystals. It also shows that only slight improvement was made for the third-pull over the second-pull with the exception of Al. Since Al exhibits a low segregation coefficient (3×10^{-2}) as compared to other metal impurities ($<10^{-5}$), the reduction of aluminum concentration to 10^{-8} from the original value in MG-Si (10^{-2}) needs at least three crystal pulling process, if other purification methods are not applied during the crystal pulling. The results shown in Table 1 are quite agreeable with this prediction.

TABLE 1

Comparison of maximum impurity concentration in 1,2 and 3-pulled ingots analyzed by spark source mass spectrometer (ppm wt)

<u>Element</u>	1 PULL		2 PULL		3 PULL	
	<u>Seed</u>	<u>Tang</u>	<u>Seed</u>	<u>Tang</u>	<u>Seed</u>	<u>Tang</u>
Cd	0.16	0.44	0.16	0.16	0.16	0.16
Mo	0.10	0.96	0.19	0.19	--	--
Zr	--	13.0	0.04	--	--	--
Cu	0.02	.05	0.01	0.02	0.01	--
Ni	0.53	19.0	0.97	0.97	0.96	1.20
Fe	2.4	560.0	0.28	0.11	0.09	0.24
Mn	0.63	29.0	0.23	0.41	0.63	0.32
Ti	0.08	120.0	0.03	0.02	0.02	0.02
Ca	--	49.0	0.37	0.38	0.20	0.56
K	--	--	0.19	0.08	--	--
Cl	2.3	2.4	0.01	0.01	0.01	0.01
P	1.6	3.7	0.74	0.74	0.45	1.20
Al	36.0	3300	5.2	8.2	0.02	0.03
Mg	0.27	36	0.05	--	0.08	0.16
Na	0.20	0.82	0.04	0.05	--	0.21
C	12.0	28	0.8	0.59	0.30	0.83
B	0.42	0.73	1.20	1.20	0.60	1.30

TABLE 2

Impurity ratio in Si ingots of each consecutive pull

<u>Element</u>	<u>1-pull/2-pull</u>		<u>2-pull/3-pull</u>	
	<u>Seed</u>	<u>Tang</u>	<u>Seed</u>	<u>Tang</u>
Cu	2	25	1	--
Fe	8.5	5.5×10^3	3	--
Mn	2.7	7.1×10^2	0.28	1.3
Ti	2.7	6.0×10^3	1.5	1
Al	6.9	4.0×10^2	2.6×10^2	2.7×10^2

3.2 Crystal Perfection

3.2.1 2-Pulled Crystals

The majority (over 75%) of the 2-pulled crystal are single crystals. Four growth facets are un-disrupted and distinctly present along the direction of crystal axis. This morphology is characteristically regarded by the crystal growers as "free-of-dislocations". X-ray topographic study revealed no dislocations at the seed end of the crystals. The etching study confirmed the X-ray work. However, wafers etched by a preferential etchant exhibit dull surfaces. Microscopic examination showed a high density of shallow etch pits on the surfaces. On the other hand, chemical etching and the X-ray studies have shown that the tang end of the "dislocation-free" crystals is not crystallographically perfect. Figure 1 shows the X-ray topograph of a silicon wafer cut from the tang end of a 2-pulled ingot. Figure 2 (a) is a higher magnification of Figure 1 taken at the center region of the wafer. This figure shows high strain field in the crystal lattice, which is primarily due to the precipitation of a second phase or impurities. Figure 2 (b) shows a higher magnification of Figure 1 taken at the periphery of the wafer. The line defects shown in this photograph are primarily dislocations.

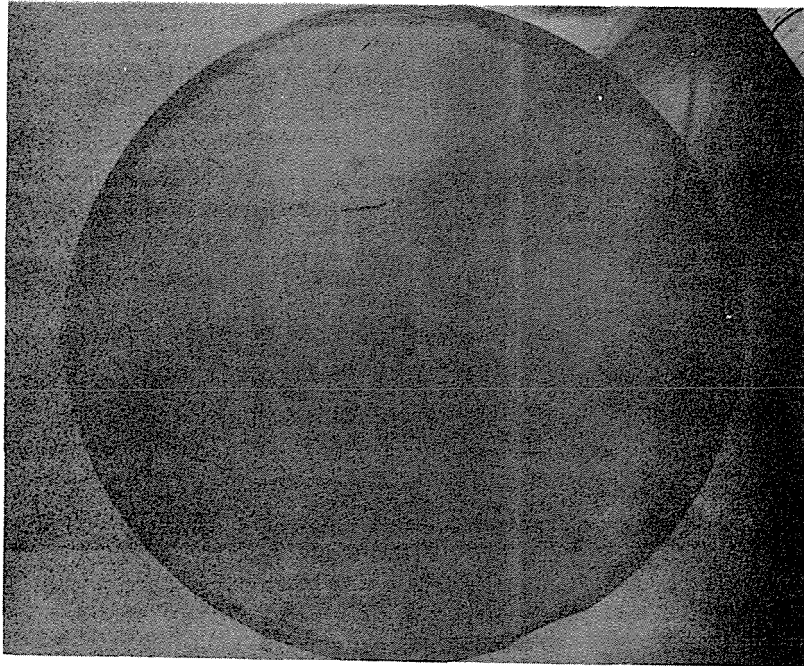
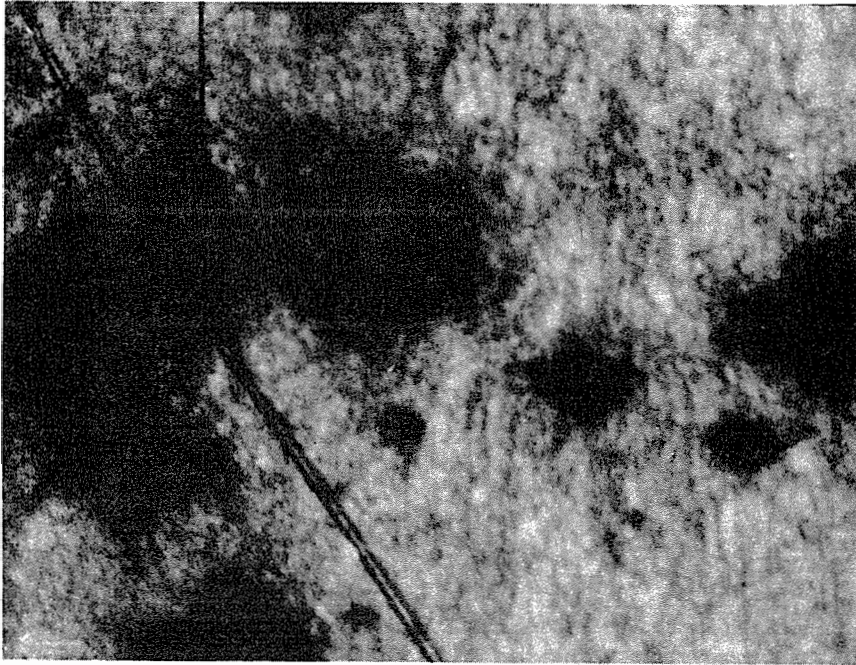
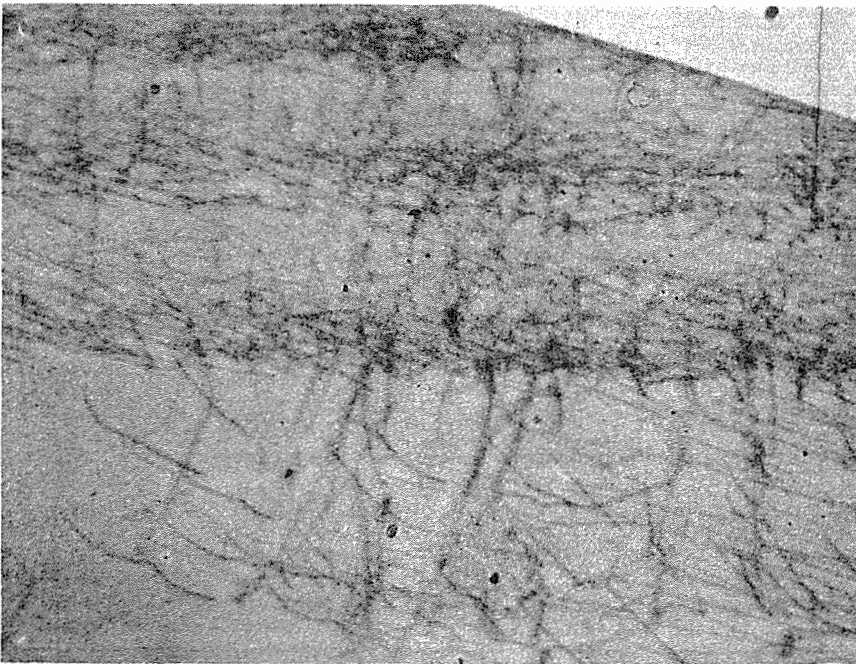


Figure 1. X-Ray topograph of a silicon wafer cut from the tang end of a 2-pulled ingot.



(a)



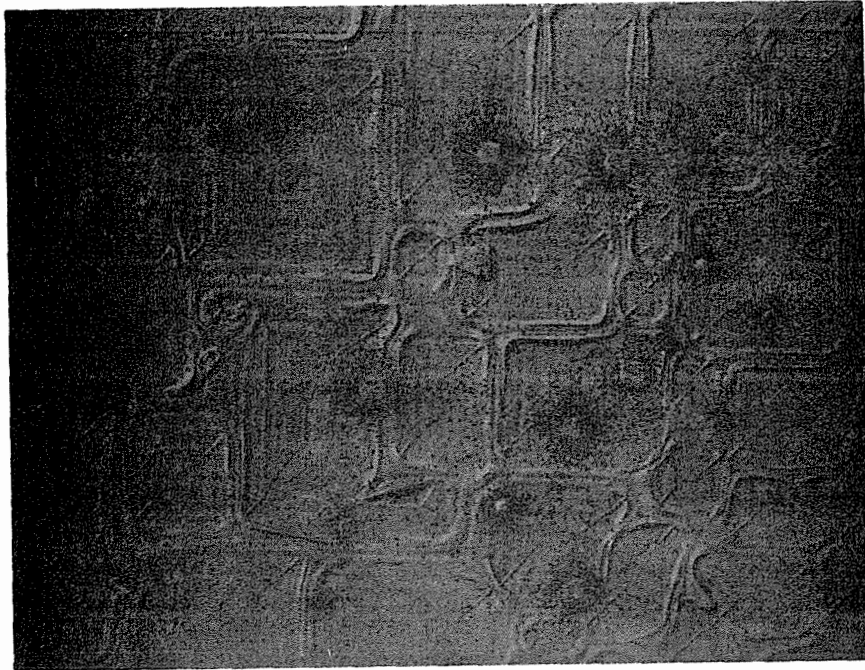
(b)

Figure 2. A higher magnification of Figure 1,
(a) center region of the wafer,
(b) periphery region of the wafer

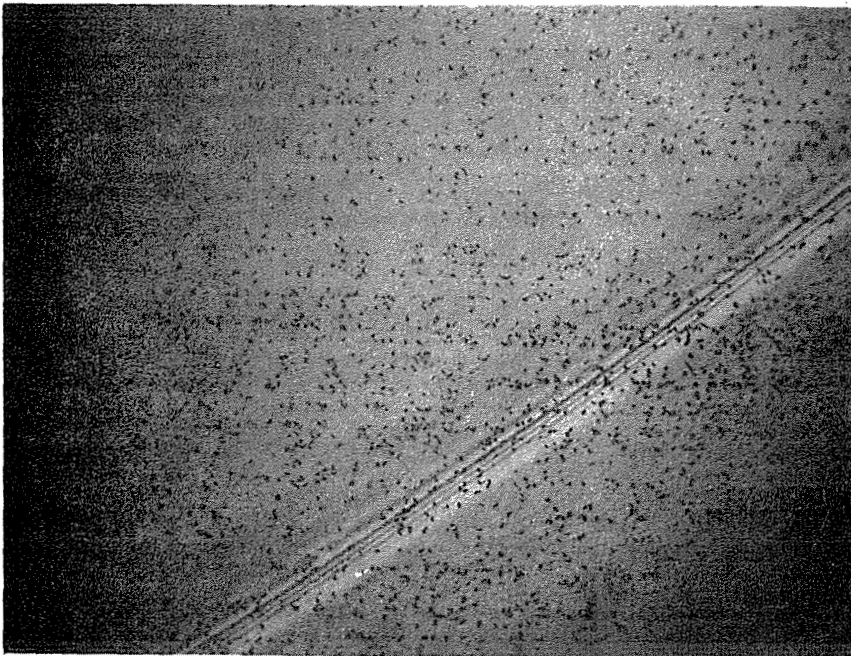
A better insight to these crystal imperfections exhibited at the tang end of 2-pulled crystals was obtained from chemical etching studies. Figure 3 (a) shows the etched surface taken from the center region of the wafer shown in Figure 1 . Three types of crystalline defects are revealed: (1) cellular cells with square or rectangular shape of irregular sizes. The formation of the cellular cells resulted from the constitutional supercooling of the melt. (2) precipitates of impurities which are located either within the cellular cells or at the edge of the cells. (3) dislocations which surround the precipitates and are manifest as small dark pits by the chemical etching. The formation of dislocations are likely due to the relief of lattice strain created by the impurity precipitates. Chemical etching reveals the same result as the X-ray topograph at the edge of wafer. Figure 3(b) shows the dislocation pits observed at the edge of the same wafer.

3.2.2 Three Pulled Crystals

Crystal perfection of the 3-pulled crystal shows considerable improvement over that of 2 - pulled crystals. Dislocation-free crystals can be consistently grown. The tang end of the 3-pulled crystals exhibit neither cellular-cell structure nor precipitates. However, the shallow etch pits still remain. Figure 4 (a) show a surface etched by Wright etch for 10 minutes followed by Sirtl etch for 3 minutes. Two types of shallow etch pits are found. One is the larger in size and distributed not uniformly. The other is smaller in size and distributed uniformly over the entire surface. The density of the small shallow etch pits approaches 10^8 cm^{-2} . This type of shallow etched pits are also observed on heavily doped semiconductor grade(S.G.) wafers as shown in Figure 4 (b).

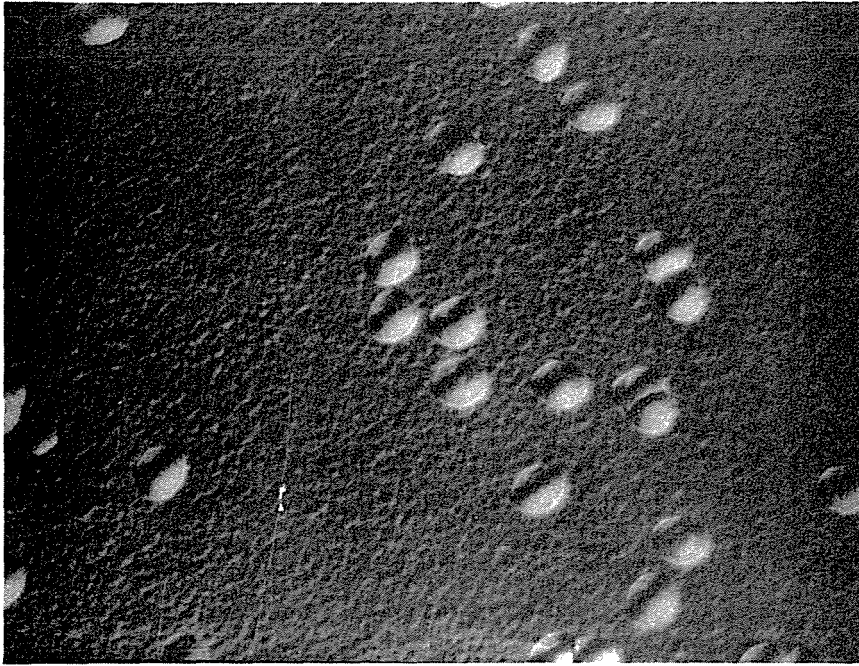


(a)

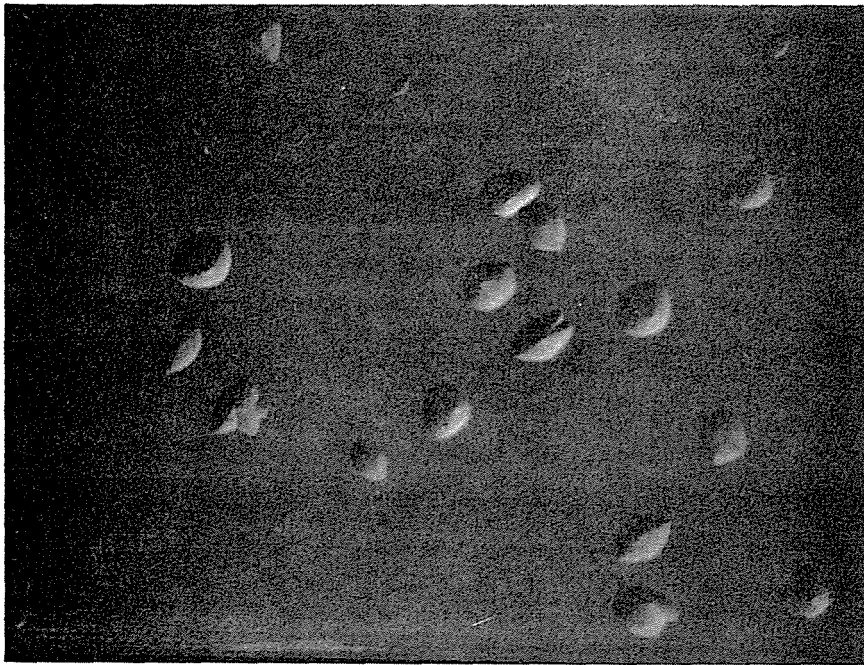


(b)

Figure 3. Etched surfaces of the wafer
shown in Figure 1
(a) center region,
(b) periphery region



(a)



(b)

Figure 4. (a) shallow etch pits observed on the wafer cut from a 3-pulled ingot.
(b) shallow etch pits observed on a S.G. wafer.

3.3 Electrical Resistivity and Carrier Mobility

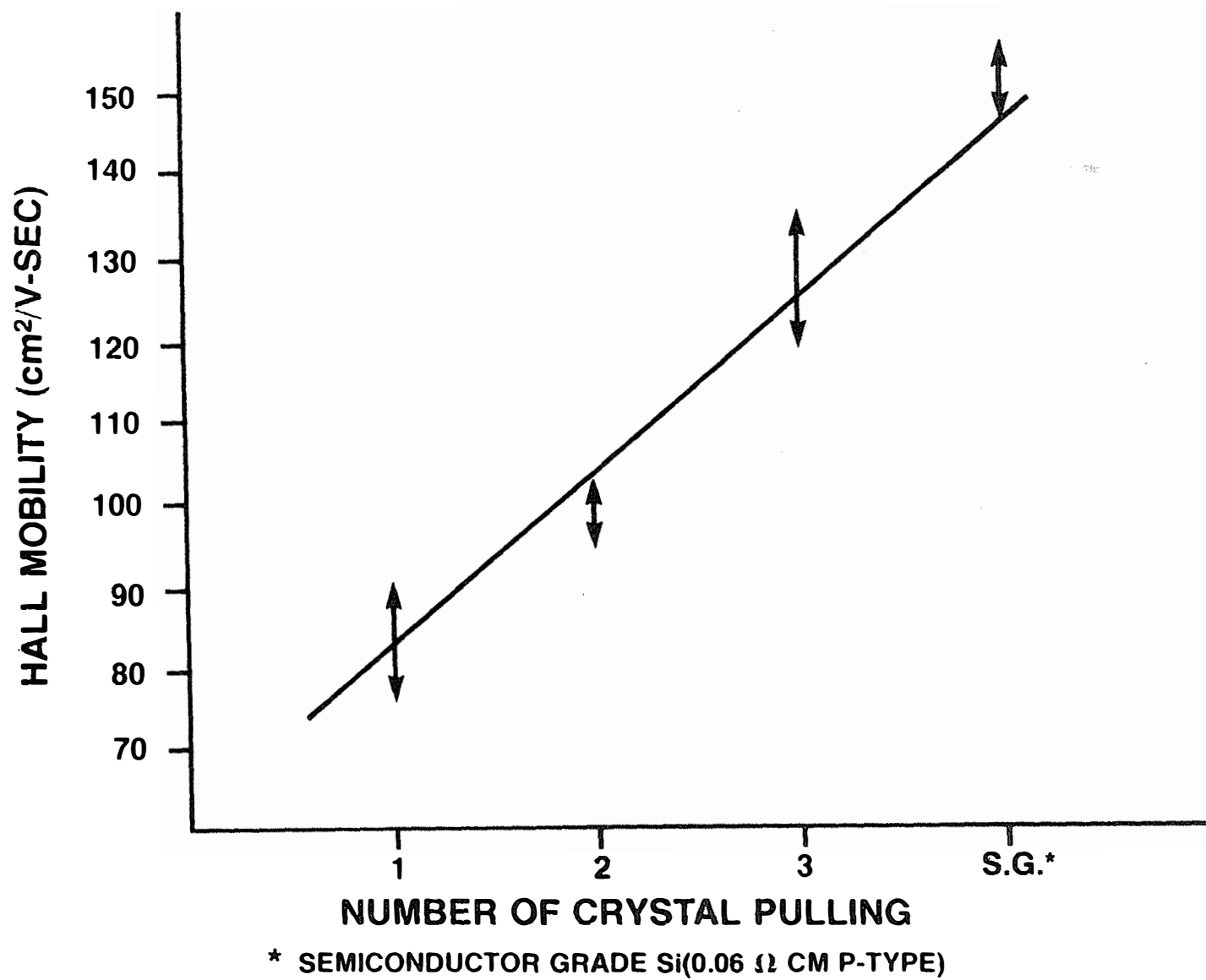
Crystals pulled from the MG-Si melts are always P-type. This confirmed by chemical analysis given in Table 1 that the sum of B and Al concentration is always greater than P concentration in crystals. The electrical resistivity for the 1-pulled crystals is always in the range of 0.04 to 0.06 Ωcm . The resistivity in the 2-pulled and 3-pulled crystals remains at 0.06 Ωcm . However, the hole mobility measured by the van der Pauw method shows that the mobility steadily increases with the number of crystal pulls (Figure 5). Typically the hole mobility in the 1-pulled crystals is in the range of 80-90 cm^2/Vsec . The mobility was increased to 100 cm^2/Vsec for 2-pulled crystals and to 120-150 cm^2/Vsec for 3-pull crystals. However, the mobility in 3-pulled crystals is still approximately 20% lower than that of the same resistivity, semiconductor-grade crystal.

3.4 Photoresponse

3.4.1 Gated Diodes

Photoresponse of the gated diodes has been tested using an iodine quartz lamp as light source. The light intensity of the lamp is equivalent to 5×10^{-3} sun. Table 3 summarizes the average values for various crystals. The I_{sc} of semiconductor grade crystals is only slightly higher than that of 3-pulled crystals. Among the 2-pulled crystals the wafers cut from the seed end of crystals give higher I_{sc} 's than that of the tang or middle portion of crystals.

Table 3 also shows that V_{oc} is apparently affected by the number of crystal pulls. However, in one case the V_{oc} of a 2-pulled crystal is as high as 3-pulled or SG crystals. The product of I_{sc} and V_{oc} increases with materials of the following order: tang or middle portion of 2-pulled crystals, seed end of 2-pulled crystals, 3 - pulled crystals, semiconductor grade crystals.



H3022

Figure 5. Plot of Hall mobility vs number of crystal pulling

TABLE 3

Average short circuit current (Isc) and open circuit voltage (Voc) for diodes illuminated under 5×10^{-3} sun

<u># Pull</u>	<u>Crystal #</u>	<u>Resistivity(Ω cm)</u>	<u>Isc(ma/cm²)</u>	<u>Voc (mv)</u>	<u>Isc X Voc</u>
2	6S	0.06	71.8	364	26.1
	10S	0.06	74.1	327	24.2
	10T	0.06	74.1	285	21.1
	24M	0.06	68.5	264	18.1
3	19S	0.06	93.1	359	33.4
	35	0.06	100.5	401	40.3
S.G.	15S	0.02	93.4	393	36.7
	2C	1.00	114.0	365	41.7

* stands for the seed end of crystals

** stands for the tang end of crystals

*** means the middle part of crystals

3.4.2 Silicon Wafers with a Shallow p-n Junction

Measurement of I_{sc} and V_{oc} was made on N^+ diffused wafers of (1) 2-pulled crystals, 2) 3-pulled crystals, and 3) semiconductor grade crystals with various resistivities. One experiment used the wafers with textured surface on the front and P^+ diffused layer on the back for the reflect field. The other experiment applied neither texturing nor back P^+ diffusion. Table 4 lists the results of the measurement for the latter one. This table shows that the improvement of 3-pulled crystals over 2-pulled crystals is primarily at I_{sc} . It also shows that the I_{sc} for all 3-pulled wafers is confined to the range between 17.27 to 18.09 ma/cm^2 , while V_{oc} is also confined to a narrow range from 0.592 to 0.602 volts. A wider range of variation of both I_{sc} and V_{oc} was observed for the semiconductor grade wafers. It is interesting to see that the semiconductor grade wafers with the same resistivity as 3-pulled crystals (i.e., $0.06 \Omega cm$) give almost identical $I_{sc} \times V_{oc}$ as those of 3-pulled crystals.

Table 5 lists the I_{sc} and V_{oc} values for wafers with a textured front surface and P^+ diffused back surface. It shows that considerable improvement of I_{sc} was made over the wafers without texture and back reflect field. The semiconductor grade wafers with the same resistivity as 3-pulled crystals have only very slight higher I_{sc} . The higher resistivity S.G. wafers, however, have much higher I_{sc} 's than that of 3-pulled crystals.

TABLE 4

Comparison of Isc and Voc of 2 and 3 pulled crystals with those
of S.G. wafers of various resistivities
(measured under AMI)

<u>Crystal</u>	<u>Resistivity</u> <u>(Ωcm)</u>	<u>Isc</u> <u>(ma/cm²)</u>	<u>Voc</u> <u>(V)</u>	<u>Isc x Voc</u> <u>(ma/cm² V)</u>
2 pull 10S	0.06	13.6	.584	7.9
10S	0.06	14.6	.585	8.6
3 pull 35	0.056	17.65	.593	10.40
40	0.060	17.27	.598	10.33
61	0.073	17.44	.592	11.02
63	0.076	17.76	.599	10.64
67	0.075	17.72	.592	10.89
93	0.076	18.09	.602	10.89
SG* 51	0.060	18.88	.578	10.9
25	0.090	21.90	.562	12.30
05	0.50	18.71	.581	11.36
49	1.20	20.82	.566	11.75
18	8.6	23.35	.536	13.21

TABLE 5

Comparison of Isc and Voc of 3-pulled N⁺ Wafers
with those of S.G. wafers of various resistivities.
(The front of wafers was textured and the back was P⁺ diffused.)

<u>Crystal</u>	<u>Resistivity</u>	<u>Isc</u> ($\frac{\text{ma}}{\text{cm}^2}$)	<u>Voc</u> (V)	<u>Isc x Voc</u>
3-pull Mg35	0.056	25.25	.542	13.69
Mg67	0.075	25.65	.544	13.95
SG 51	0.060	25.72	.549	14.12
05	0.50	29.7-	.565	16.78
49	1.20	29.03	.559	16.23
18	18.0	31.10	.505	15.71

3.4.3 Epitaxy Wafers with a P-N Junction

Table 6 shows I_{sc} and V_{oc} of the N^+ diffused epitaxy layers on the various substrates. It shows that very little difference was observed from the substrates of the 2-pulled or 3-pulled crystals. The epitaxy layers deposited on the semiconductor grade substrate do not give a significantly better I_{sc} and V_{oc} than those deposited on 2-pull substrate.

3.4.4 $I_{sc} \times V_{oc}$ Product and Predicted Maximum Cell Efficiency

The data given in Tables 4 and 6 can be used to predict the maximum solar cell efficiency. Two assumptions were made: (1) The field factor is assumed constant (0.75). (2) 3% is added to the solar cell efficiency of both the texture surface and back reflect field are applied. Based on these assumptions, a plot of cell efficiency vs $I_{sc} \times V_{oc}$ was made and shown in Figure 6 for the use of various materials. The straight line indicates the linear proportionality between the cell efficiency and $I_{sc} \times V_{oc}$. Three dotted loops are shown along the straight line of the plot. The loop at the lower region of the straight line consists of the data points of 2-pulled crystals. The loop at the middle region of the line consists of the data points of 3-pulled crystals. The loop at the upper region is primarily the data points of epitaxial structure or the high resistivity (0.09 $\Omega\text{-cm}$) semiconductor grade substrates.

4. DISCUSSIONS

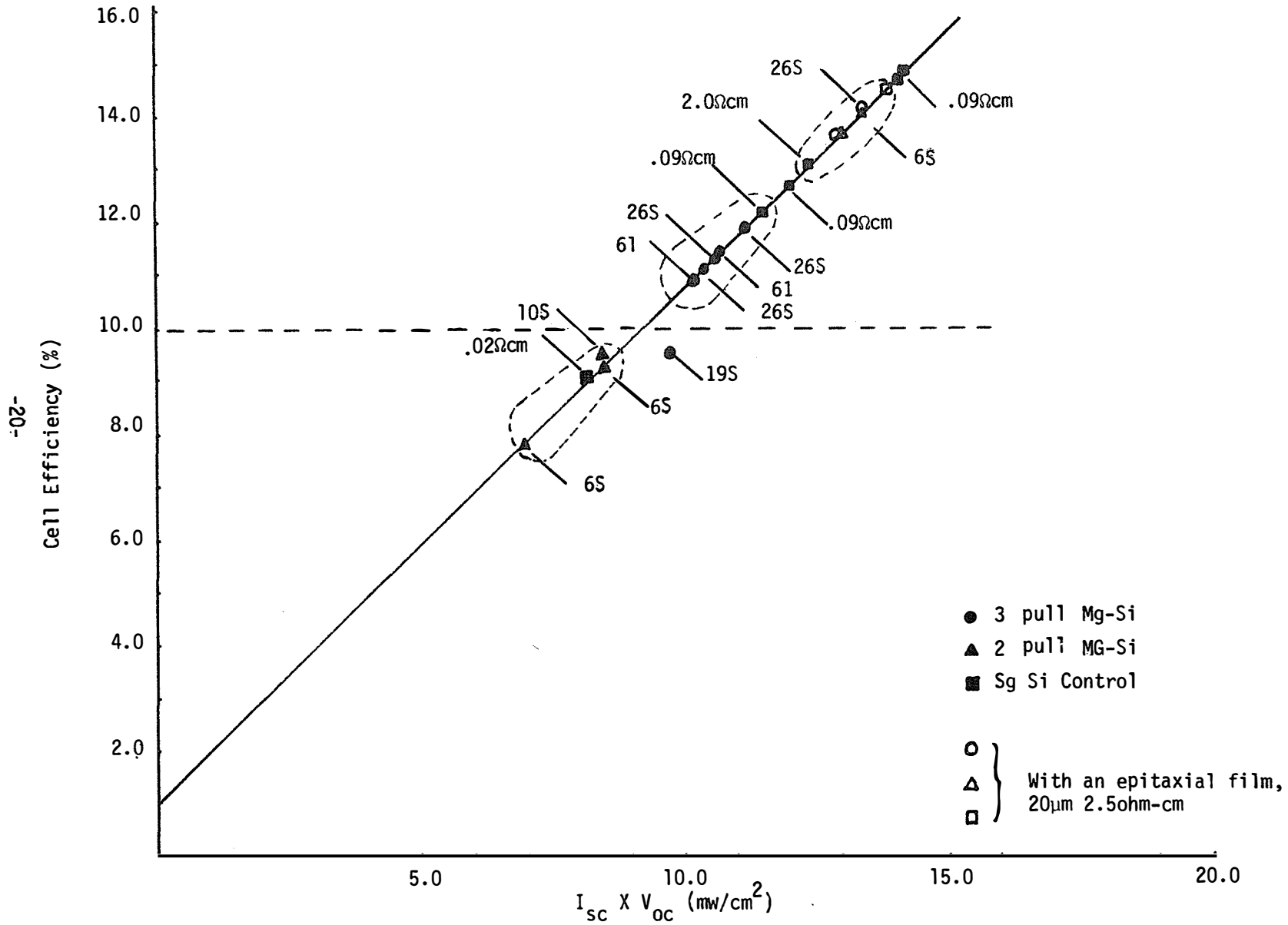
The present study has reconfirmed that the crystal pulling is an effective method of removing metallic impurities from silicon. This is clearly seen by comparing the impurity concentration in metallurgical-grade silicon with the 1-pulled crystals, or comparing the 1-pulled crystals with 2-pulled crystals.

TABLE 6

Isc and Voc of N⁺ diffused wafers (2" dia.)
with an Epitaxial layer on the substrates
of various numbers of crystal pulling

<u>Substrate</u>	<u>Isc(ma/cm²)</u>	<u>Voc(V)</u>	<u>Isc Voc</u>
2-pull 6S	22.2	.573	12.8
10S	21.7	.567	12.3
3-pull 19S	22.2	.582	13.0
26S	27.2	.566	12.6
S.G. (0.02 cm)	21.7	.599	13.0
(1.0 cm)	22.8	.559	12.7

Figure 6. Plot of cell efficiency vs $I_{sc} \times V_{oc}$ for various materials.



The slight impurity difference between the 2-pulled and 3-pulled crystals is primarily due to (1) the sensitivity of the analytical instrument, or (2) the contamination to 3-pulled crystals during the material processing. The structural and electrical characterization of the crystals confirm that the steady improvement of crystal quality by the additional crystal pulling.

The 1-pulled crystals which were used as feedstock for the second crystal pulling contain a lamellar structure at the tang end. The transition from polygonal grain structure to lamellar structure accompanies an increase in impurity concentration of 2-3 orders of magnitude¹⁻². If the portion of the lamellar structure is eliminated for use as feedstock, the purity in the 2-pulled crystals should be improved considerably. It seems likely that it may need only 2 crystal pulling steps to purify metallurgical grade silicon to semiconductor grade quality. This may not be difficult to realize since the recent separate study has developed techniques to grow large grain 1-pulled crystals with considerable extended length.

The high density shallow etch pits existed in the 2-and 3-pull crystals is a unique feature of this material. The shallow etch pits may be likely resulted from the impurity complexes, although the chemical and electrical data were not able to verify this speculation. The high density of the shallow etch pits lead to the dull surfaces, which can be regarded as "cosmetic defects".

The primary limitation of this process is the ineffective removal of impurities with low segregation coefficients, e.g., boron, oxygen and germanium. The presence of oxygen and germanium in silicon will not seriously affect the silicon quality. This is because both are electrically in-active and do not contribute to the deep energy levels in the bandgap. However, the existence of boron in the range of five ppm seriously limits the usage of this material to heavy-doped P-type applications.

REFERENCES

1. H.M. Liaw and Frank Secco d'Aragona, Quarterly Report, DOE/SERI-8-119-3/2 Aug. (1980).
2. Frank Secco d'Aragona, H.M. and Liaw D.M. Heminger, "Materials and New Processing Technologies for Photovoltaics" Eds. J.A. Amick, P. Rai-Chouchury, E. Sirtl, and J.P. Dismukes, Electrochem. Soc. (1981).